A Self-Decoupled Antenna Array Using Inductive and Capacitive Couplings Cancellation

Jiangwei Sui, *Member, IEEE*, and Ke-Li Wu, *Fellow, IEEE*

***Abstract*— The concept of a self-decoupled antenna array using the cancellation of two opposite couplings is proposed in this article. A pair of such antennas can be closely placed with inherent high isolation without using an extra decoupling structure between the antennas. A pertinent equivalent circuit model is presented to illustrate the physical mechanism of this new concept. It is found that the inductive and capacitive couplings between the antennas can be well canceled out with each other by properly adjusting the antenna dimensions. A demonstrating antenna array with a spacing of $0.024\lambda_0$ at the working frequency of 3.5 GHz and its counterpart array are first studied. The measured results show that although the proposed antenna array occupies a slightly larger size than its counterpart array, it presents better performance compared with its counterpart antenna array in port isolation (from 10 to 20 dB), total efficiency (from 68% to 80%), and envelope correlation coefficient (ECC) (from 0.14 to 0.04) throughout the desired frequency band of 3.3–3.8 GHz. A 3-D self-decoupled antenna array is designed to show that the proposed antenna can be in a compact form factor. Another self-decoupled array and its counterpart working at 2.14 GHz (long-term evolution (LTE) band 1) are studied through multi-input multi-output (MIMO) over-the-air (OTA) test when the arrays are integrated with an LTE module, showing significant improvement on the data throughput.**

***Index Terms*— Antenna array, couplings cancellation, isolation, multi-input multi-output (MIMO), mutual coupling, over the air (OTA), self-decoupled, throughput.**

I. Introduction

MULTI-INPUT multi-output (MIMO) technology, by adopting multiple antennas to carry different data streams in the same frequency band, has been widely used in wireless communication systems for increasing the data throughput. However, due to the compact volume of a wireless terminal, strong electromagnetic (EM) coupling may exist among antennas, which severely diminishes the MIMO performance [1]. It is shown in [2] from both theory and experiment that 20 dB isolation is required for MIMO antennas in terminal applications to achieve satisfactory system performance. To obtain such high isolation, the spacing between antennas needs to be large enough, usually a quarter wavelength [3], which is not available in most terminal applications. Such predicament will be more severe when the antenna number becomes large in future wireless communication systems [4].

In previous works, various techniques have been proposed to mitigate the mutual coupling between closely spaced antennas. A category of these techniques is to ingeniously introduce a decoupling structure between the two coupled antennas. Such structures include an electromagnetic bandgap (EBG) structure [5], a defected ground structure (DGS) [6], a parasitic scattering element [7]–[9], a transmission line circuit [10], [11], a neutralization line [12], [13], an *LC* circuit [14], [15], a coupler [16], a coupled-resonator circuit [17], [18], a split ring [19], and capacitive loads [20].

Although these techniques are effective to improve the isolation, they all require introducing extra auxiliary structures or circuits between or on the coupled antennas. Very recently, two gap-coupled loop antennas are asymmetrically placed to achieve inherent isolation, without introducing a decoupling structure [21]. However, its achieved lowest isolation throughout the band of 3.4–3.6 GHz is only about 10 dB. A special antenna element containing a T-shaped feeding element and two identical L-shaped radiating elements is proposed in [22], to achieve more than 20 dB isolation by increasing the antenna spacing and confining the current distribution to the exciting antenna. An innovative orthogonal-mode method is proposed in [23], to mitigate the mutual coupling between a bent monopole and an edge-fed dipole antenna. However, this method only applies to two antennas of different antenna types and the achieved matching condition is only about -6 dB.

In this article, a new concept for antenna array design called self-decoupled antennas is proposed. By employing the concept, the antenna element is designed to adjust the inductive and capacitive couplings between the two antennas, leading to inherent decoupling without using extra decoupling structures between antennas, such as EBG, DGS, parasitic elements, and a decoupling network. The working mechanism behind this concept is to balance the inductive and capacitive couplings between antenna elements. Through the appropriate design of the antenna structure and dimensions, these two opposite couplings can be well canceled out with each other in a wide frequency band, although the eventual antenna array design may occupy a slightly larger size or own more complex configuration than the traditional antenna array.

The working mechanism of the proposed self-decoupled antenna array concept is explained using an equivalent circuit in Section II. The EM and equivalent-circuit simulated

Manuscript received March 7, 2019; revised January 19, 2020; accepted February 16, 2020. Date of publication March 9, 2020; date of current version July 7, 2020. This work was supported in part by the Research Grants Council of the Hong Kong Special Administrative Region, China, under Grant 14205217. *(Corresponding author: Ke-Li Wu.)*

Jiangwei Sui was with the Department of Electronic Engineering, The Chinese University of Hong Kong, Hong Kong. He is now with Vivo Communication Technology Company, Ltd., Dongguan 523000, China (e-mail: suijwmyy@gmail.com).

Ke-Li Wu is with the Department of Electronic Engineering, The Chinese University of Hong Kong, Hong Kong (e-mail: klwu@cuhk.edu.hk).

Color versions of one or more of the figures in this article are available online at http://ieeexplore.ieee.org.

Digital Object Identifier 10.1109/TAP.2020.2977823

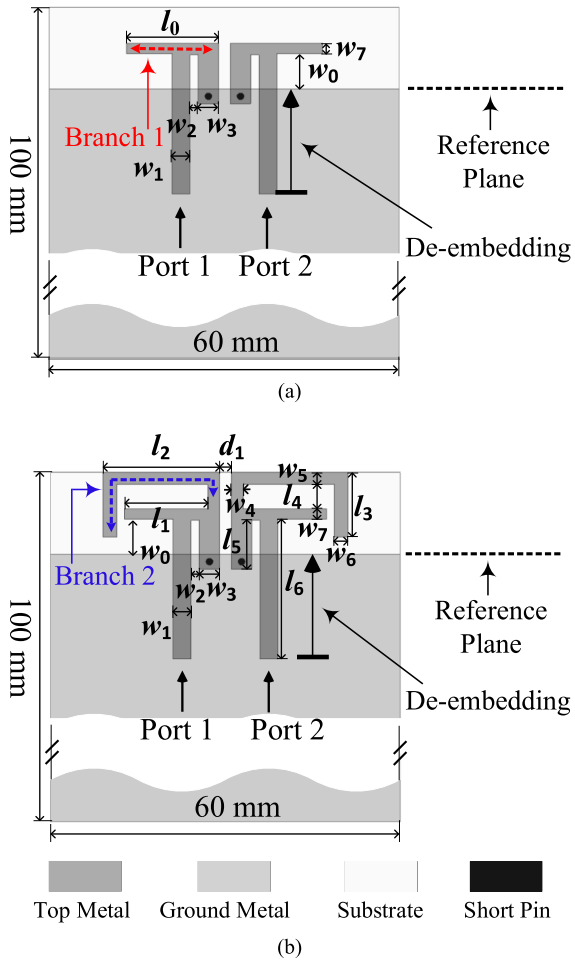

Fig. 1. Configurations of two two-element arrays working at 3.5 GHz. (a) Conventional IFA array. (b) Proposed self-decoupled array.

S-parameters show very good agreement in both magnitude and phase, validating the proposed concept. Three demonstration examples are presented in Section III, showing a performance improvement compared with their conventional counterparts not only in port isolation, total efficiency, and envelope correlation coefficient (ECC) but also in measured MIMO data throughput. Finally, the conclusion is given in Section IV.

II. Antenna Configuration and Working Mechanism

A. Antenna Configuration

Fig. 1(a) shows the configuration of two conventional inverted-F antennas (IFAs) working at 3.5 GHz as the counterpart of the proposed self-decoupled antennas. This IFA element has one radiating arm, marked as Branch 1. For the proposed self-decoupled antenna element, one more branch marked as Branch 2 is added to the IFA element over the radiating arm, as is shown in Fig. 1(b). Two identical such antenna elements are placed back-to-back, with the dimensional parameters listed in Table I. The PCB substrate for printing the antenna prototype is 1.6 mm thick FR4 with a relative permittivity of 4.3 and loss tangent of 0.02.

TABLE I

Dimensions of the Two Antenna Arrays at 3.5 GHz (Unit: mm)

l_0	16.2	l_4	4.2	w_1	3.1	w_5	2
l_1	14.2	l_5	8.3	w_2	1.4	w_6	2.3
l_2	20	l_6	24	w_3	3.5	w_7	1.8
l_3	11	w_0	6	w_4	2	d_1	2

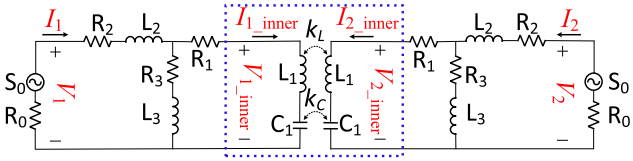

Fig. 2. Proposed equivalent circuit for a self-decoupled antenna array and its conventional IFAs counterpart seen from the reference plane shown in Fig. 1.

B. Working Mechanism

The working mechanism of this proposed antenna design concept is explained using an equivalent circuit. There are two kinds of couplings between a pair of coupled antennas, more or less. Without deliberate manipulation, the two couplings will not cancel out each other. With the proposed method, the two couplings are intentionally tuned to be at the same magnitude, making them cancel out each other. The equivalent circuit model of the self-decoupled antenna array is illustrated in Fig. 2. It is noted that this circuit model corresponds to the two antennas whose feeding lines have been deembedded, as shown in Fig. 1, indicating that the reference plane is moved forward to the antenna radiating body. Two coefficients k_L and k_C are introduced to describe the inductive and capacitive coupling characteristics of the two antennas. Here, k_L and k_C are the relative coupling coefficients between two inductors and two capacitors, respectively. The coupling circuit is framed in Fig. 2 using a dotted blue box. As is denoted in Fig. 2, it is easy to prove that the total mutual impedance Z_{21} of the two antennas can be decoupled if the mutual impedance Z_{21_inner} defined by the framed coupling circuit vanishes. The mutual impedance of the circuit can be found as

$$Z_{21\_inner} = j\left(\omega L_1 \cdot k_L - \frac{1}{\omega C_1} \cdot \frac{k_C}{1-k_C^2}\right) \tag{1}$$

where j is the imaginary sign and ω is the radian frequency. Formula (1) implies that the mutual impedance Z_{21} can be canceled out for a given frequency by adjusting the four parameters L_1, C_1, k_C, and k_L. By curve fitting, the corresponding values of the circuit elements for the two antenna arrays shown in Fig. 1 are listed in Table II, resulting in $Z_{21\_inner} = -\text{j}0.019\ \Omega$ for the self-decoupled array at the center frequency 3.5 GHz, showing good cancellation between the two different couplings.

The simulated S-parameters of the equivalent circuit and the EM models for these two antenna arrays are compared in Fig. 3. It is found that both the magnitudes and phases of the S-parameters between the circuit and EM models agree very well. The good agreement indicates that there exists a correspondence between the physical model and the circuit model. To save space, only three crucial parameters, w_4, l_1, and l_4 are discussed here.

TABLE II

CIRCUIT PARAMETER VALUES FOR THE TWO ANTENNA ARRAYS

	R_1	R_2	R_3	L_1	L_2	L_3	C_1	k_L	k_C	Z_{21_inner} @3.5GHz
Conventional IFA array	0.9	19	1.3	0.94	2.48	1.74	1	0.37	0.08	j3.99
Self-decoupled array	1.6	19	2.4	0.46	1.9	1	1.78	0.55	0.209	-j0.019

* The unit is Ω for R_1, R_2, R_3 and Z_{21}, nH for L_1, L_2 and L_3, and pF for C_1.

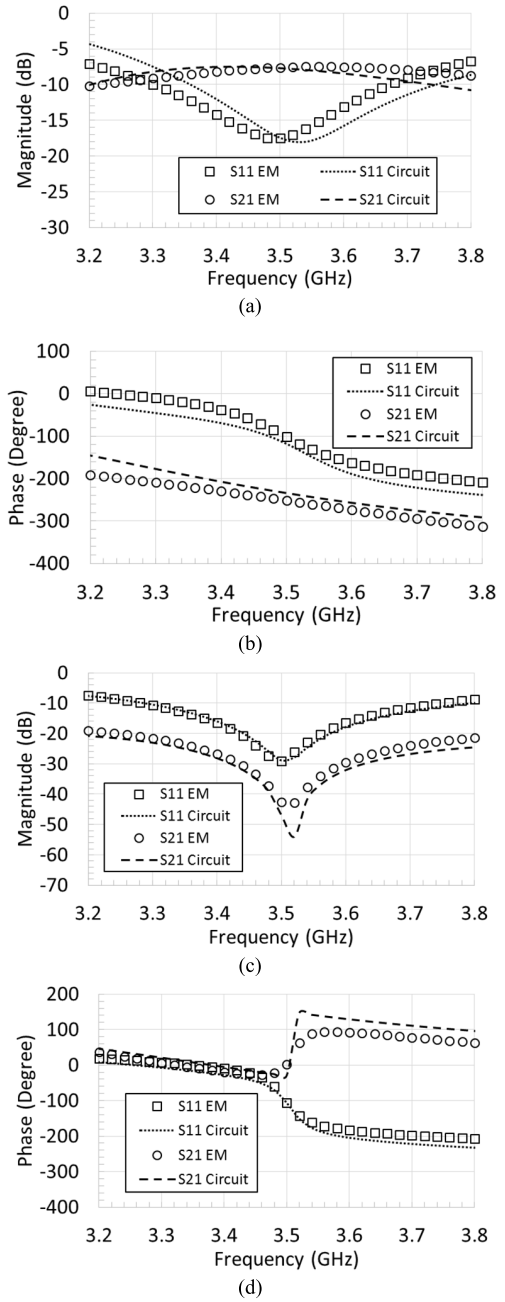

Fig. 3. Comparison of the simulated S-parameters by the circuit and EM models for the two antenna arrays. (a) Magnitude of the conventional IFAs. (b) Phase of the conventional IFAs. (c) Magnitude of the self-decoupled antennas. (d) Phase of the self-decoupled antennas.

The effect of w_4 on the S-parameters of the antennas is presented in Fig. 4. It is seen that mutual coupling $|S_{21}|$ can be easily tuned by adjusting w_4 without deteriorating

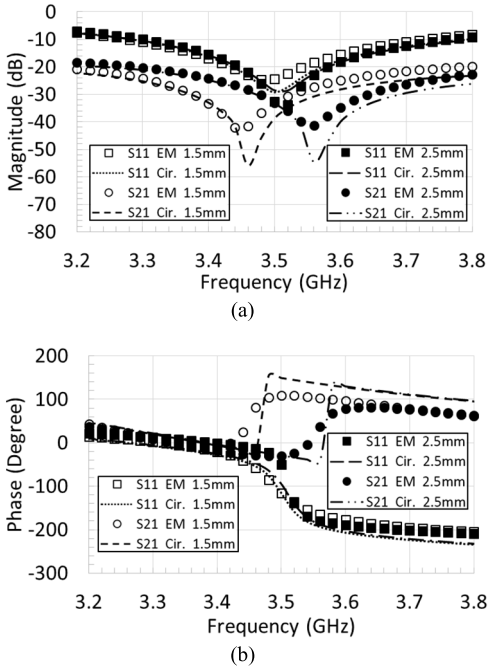

Fig. 4. Comparison of S-parameters between equivalent circuit and EM simulations for the self-decoupled antennas with different w_4. (a) Magnitude. (b) Phase. When w_4 changes from 2 to 1.5 and 2.5 mm in EM simulation, only C_2 changes from 0.209 to 0.2035 and 0.2145 in the equivalent circuit simulation, respectively.

TABLE III

CIRCUIT ELEMENT VALUES FOR DIFFERENT PHYSICAL DIMENSIONS

	R_1	R_2	R_3	L_1	L_2	L_3	C_1	k_L	k_C	Z_{21_inner} @3.5GHz
w_4=1.5 mm	1.6	19	2.4	0.46	1.9	1	1.78	0.55	0.2035	j0.14
w_4=2.5 mm	1.6	19	2.4	0.46	1.9	1	1.78	0.55	0.2145	-j0.18
l_1=14 mm	1.7	18	2.55	0.41	1.88	0.99	1.82	0.6	0.2125	-j0.15
l_1=14.4 mm	1.5	18	2.35	0.55	2	1.05	1.7	0.48	0.207	-j0.021
l_4=3.7 mm	1.5	18	2.35	0.51	2	1.04	1.67	0.48	0.191	-j0.014
l_4=3.2 mm	1.5	1.8	2.35	0.5	2	1.07	1.65	0.55	0.206	j0.119

* The unit is Ω for R_1, R_2, R_3 and Z_{21}, nH for L_1, L_2 and L_3, and pF for C_1.

the matching condition $|S_{11}|$ too much. The corresponding equivalent-circuit simulated results are also presented in Fig. 4 with detailed element values listed in Table III, which shows that a 0.5 mm increase of w_4 corresponds to a 0.0055 increase of k_C with other element values untouched, presenting an independent correspondence.

It is seen from Fig. 5(a) that the working frequency of the self-decoupled antennas decreases as l_1 increases. This is understandable because l_1 is the length of the radiating arm of the conventional IFAs. The effect of the distance between the two branches shown in Fig. 1, l_4, is studied in Fig. 5(b). It is found that when l_4 decreases, the matching bandwidth will become slightly narrower and the isolation frequency will be shifted to a lower frequency. The corresponding element values

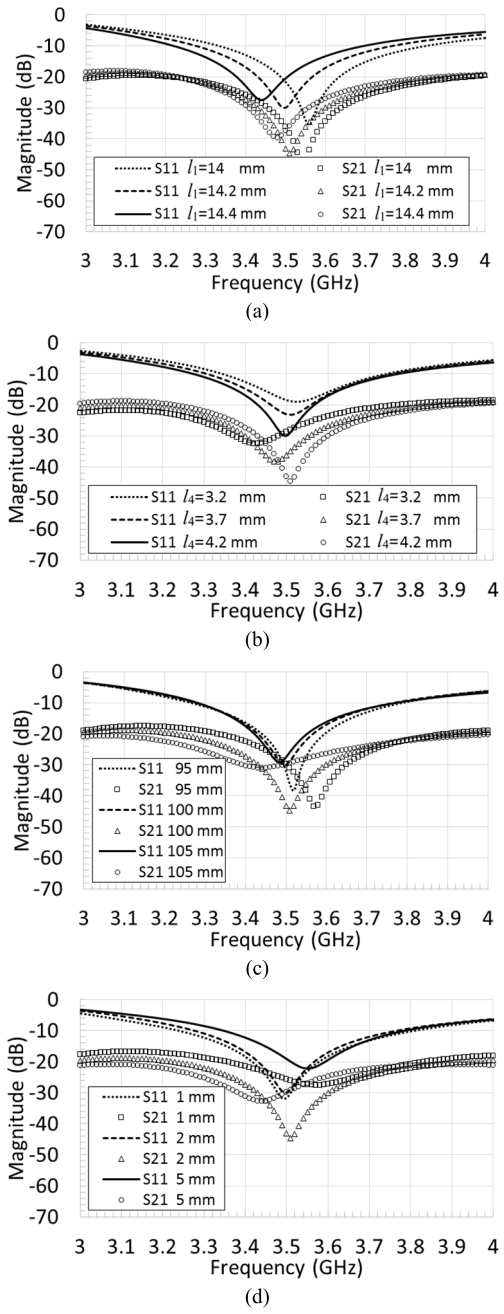

Fig. 5. Simulated S-parameters versus physical dimensions of (a) l_1, (b) l_4, (c) l_0, and (d) d_1.

for these different physical dimensions are listed in Table III. It clearly shows that, although the two coupling coefficients, k_L and k_C, both vary when changing l_1 or l_4, the overall mutual impedance, Z_{21}, will maintain a small value, indicating a good cancellation of these two different couplings.

It is also found through EM simulation that the decoupling effect is not sensitive to the ground size and antenna spacing, showing good robustness of the proposed self-decoupled antenna array, as shown in Fig. 5(c) and (d).

In sum, the major design steps include the following.

1) Designing a proper l_1 to achieve a good return loss at the desired frequency.

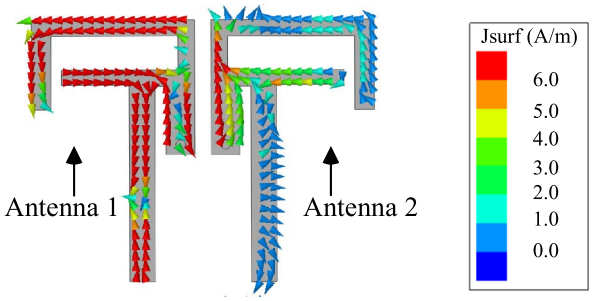

Fig. 6. Simulated current distribution of the proposed self-decoupled antennas.

Fig. 7. Photographs of the proposed self-decoupled antenna array working at 3.5 GHz. (a) Top view. (b) Bottom view. (c) Measurement setup in the anechoic chamber.

2) Choosing a proper w_4 to get good isolation at the desired frequency.
3) Fine-tuning l_4 and other parameters to enhance matching and isolation.

To better understand the physical mechanism of the inherent mutual coupling cancellation, the simulated current distribution of the proposed self-decoupled antenna array at 3.5 GHz is presented in Fig. 6. In the simulation, antenna 1 is excited while antenna 2 is terminated with a 50 Ω load. It is seen that the current flowing into port 2 is well mitigated, which ensures the inherent self-cancellation of the couplings between the proposed antennas.

A fact that should be mentioned here is that the equivalent circuit is only used to illustrate the working principle of a pair of self-decoupled antennas. It is not necessary to have an equivalent circuit for tuning the two couplings. One can always tune the antenna dimensions directly with EM simulation.

III. Demonstration Examples

In this part, two demonstration examples are presented. First, the two antenna arrays working at 3.5 GHz, which are presented in Fig. 1 and Table I to illustrate the working mechanism, are fabricated and measured. Second, to study the MIMO over-the-air (OTA) performance, two other antenna arrays working at 2.14 GHz (long-term evolution (LTE) band 1) which can be supported by a commercial LTE MIMO module are studied.

A. Antenna Array Working at 3.5 GHz

Fig. 7 shows some photographs of the proposed self-decoupled antenna array that is discussed in Section II. The simulated and measured S-parameters of these two

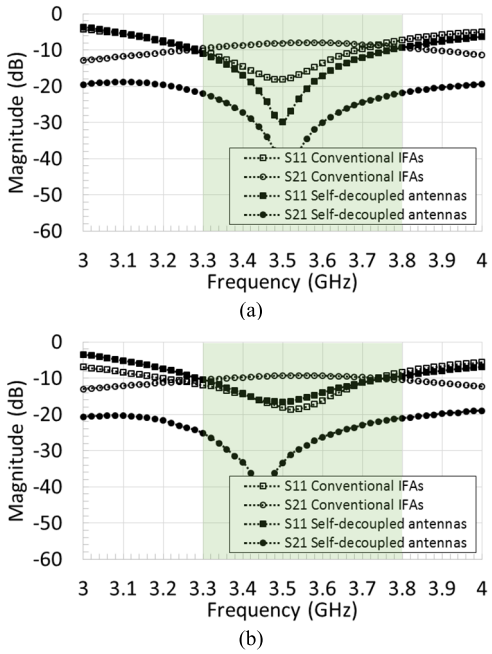

Fig. 8. S-parameters of the conventional IFAs and the self-decoupled antenna array described in Fig. 1 and Table I. (a) EM simulated. (b) Measured.

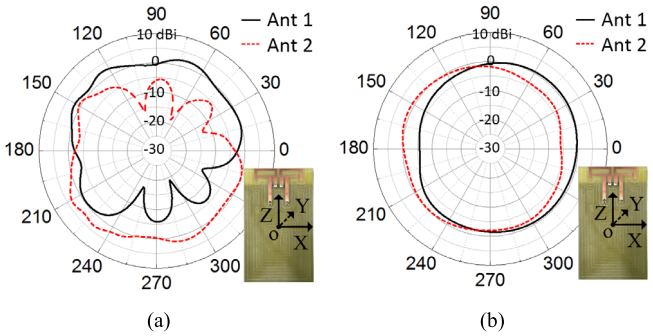

Fig. 9. Measured radiation patterns of the proposed self-decoupled antenna array. (a) *xoz* plane. (b) *xoy* plane. Ant 1 denotes the left antenna and Ant 2 denotes the right antenna.

antenna arrays are compared in Fig. 8. It is observed that in the frequency band of 3.3–3.8 GHz, the measured isolation is enhanced from about 8 dB to better than 20 dB using the proposed self-decoupled concept, whereas S_{11} is maintained to be lower than -10 dB throughout the band.

The radiation performance of the two antenna arrays is studied in an ISO17025 accredited anechoic chamber. During measurement, when one antenna is excited, the other antenna is terminated with a matched load. It is seen from Fig. 9 that at both the *xoz* and *xoy* planes, the total gain patterns of the antennas with different port excitation are complementary with each other, which hints that the proposed antenna array has good diversity characteristics. Fig. 10 shows the measured total efficiency of the two antenna arrays from 3.3 to 3.8 GHz. The average total efficiency throughout the frequency band is about 68% for the conventional IFAs and about 80% for the self-decoupled antennas, showing a significant improvement.

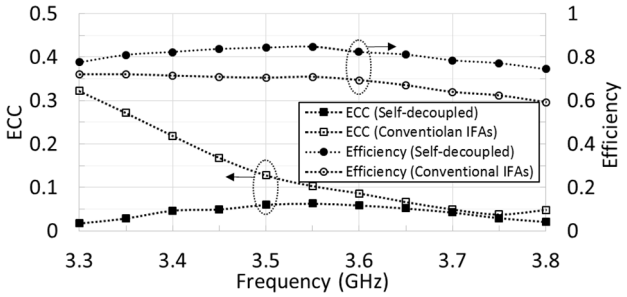

Fig. 10. Measured total efficiency and ECC of the conventional IFAs and the self-decoupled antennas described in Fig. 1 and Table I.

TABLE IV
COMPARISON WITH SOME PRIOR WORKS

Ref.	Physical Connection Requirement	20 dB Isolation Bandwidth (%) [1]	Matching Circuit Requirement	Working Mechanism
[9][2017]	No	6	No	Parasitic Element
[17][2014]	Yes	12.2	Yes	Decoupling Network
[19][2017]	Yes	24	Yes	Split Ring
[22][2019]	No	5.7	No	Current Confinement
[23][2018]	No	5.7 [2]	Yes	Orthogonal Mode
This work	No	14	No	Couplings Cancellation

[1]The 20 dB isolation bandwidth is calculated under the condition that the return loss |S11| is better than 10 dB. (2) The bandwidth in [23] is calculated under the condition that the return loss is better than 6 dB.

The ECC between two antennas is studied to evaluate the correlation attribute of the two antenna arrays. Following the method presented in [24], ECC can be calculated using the measured 3-D far-field electric fields. As shown in Fig. 10, the average ECC for the two conventional IFAs is about 0.14 throughout the band, whereas that for the two self-decoupled antennas is 0.04, showing a significant ECC reduction.

To have a clearer view of the proposed self-decoupled concept, the self-decoupled antenna array discussed above is compared with some prior works in Table IV from several key aspects, including physical connection requirement between antenna elements, fractional bandwidth for 20 dB isolation, matching circuit requirement, and working mechanism. Compared with the antennas in [17] and [19], this self-decoupled antenna does not require the antenna elements to be physically connected, which will be more convenient and flexible for antenna design and implementation in a practical terminal. Moreover, this self-decoupled concept will not deteriorate the matching condition after decoupling so that it does not require a matching circuit to recover the matching condition, reducing the complexity and cost of the whole design. Above all, the most distinct feature of this self-decoupled antenna array is its working mechanism, which utilizes the cancellation of

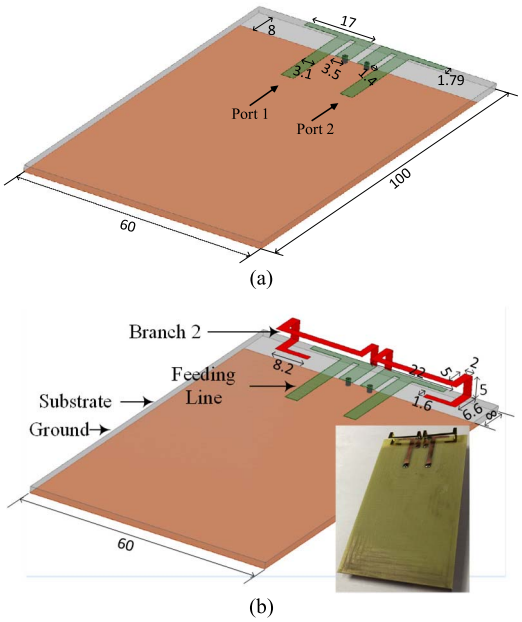

Fig. 11. Configurations and dimensions (in mm) of the 3-D antenna arrays. (a) Conventional IFAs. (b) 3-D self-decoupled antenna array with a prototype picture inserted in.

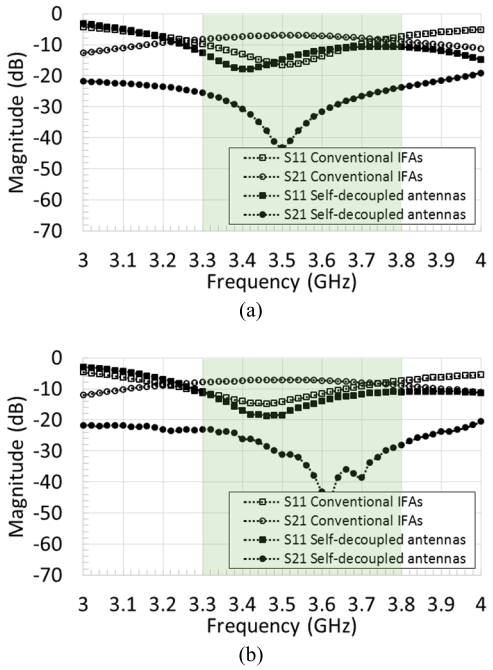

Fig. 12. S-parameters of the 3-D self-decoupled antenna array and its IFA counterpart. (a) Simulated. (b) Measured.

two different kinds of couplings existing between the antenna elements.

The occupied size of the antenna array should be mentioned here. Compared with its counterpart array, since Branch 2 is introduced to tune the two kinds of couplings, its occupied size is slightly larger than that of the traditional counterpart array.

B. Antenna Array Working at 3.5 GHz With 3-D Geometry

As discussed in the last example in Part-A, the occupied size of the proposed array is larger than its traditional counterpart after Branch 2 is introduced. A 3-D implementation of Branch 2 can effectively reduce the required clearance.

In this example, as shown in Fig. 11, the real estate for both the proposed 3-D antenna array and its counterpart are the same, which is 8 mm. The height of Branch 2 is 5 mm, which is common to most practical scenarios. A photograph of the prototyped 3-D antenna array is inserted in Fig. 11(b).

The EM simulated and measured S-parameters are given in Fig. 12. It is seen that the isolation is better than 20 dB with the 3-D self-decoupled array, whereas that of the traditional counterpart is only about 8 dB throughout the band of 3.3–3.8 GHz. It is interesting to see that −10 dB matching bandwidth of the self-decoupled array is wider than that of its counterpart without any matching network.

C. Antenna Array Working at 2.14 GHz

In order to study the impact of reducing mutual coupling and improving the total efficiency on the MIMO performance, the second case study involves a pair of self-decoupled antennas and its conventional IFA counterpart working in LTE band 1 (2.11–2.17 GHz).

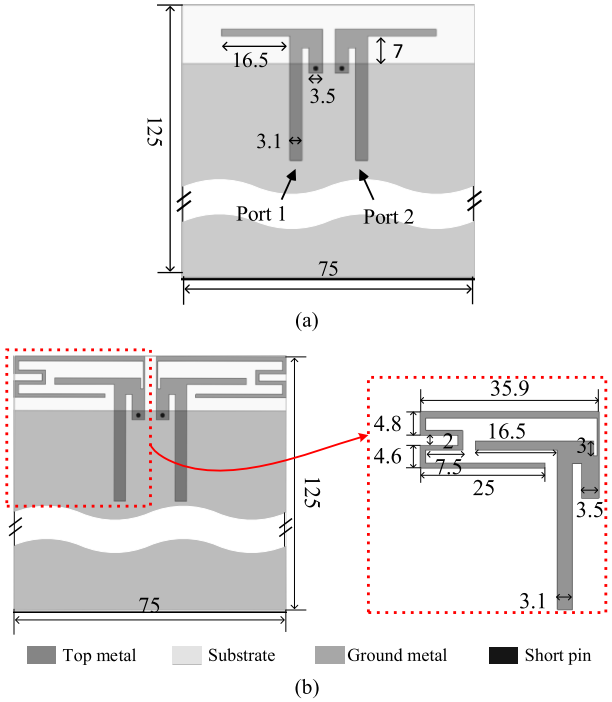

Fig. 13. Configurations and dimensions (in mm) of two antenna arrays working at 2.14 GHz for MIMO OTA test. (a) Conventional IFAs. (b) Self-decoupled antenna array.

Fig. 13 shows the configurations of the third self-decoupled antenna array and its conventional IFAs counterpart. To save space, only the measured S-parameters of these two antenna arrays are presented in Fig. 14. It is seen that the isolation at the center frequency of 2.14 GHz is enhanced from about 10 dB for the conventional IFAs to about 25 dB for the self-decoupled antenna array, whereas the matching condition is better than −10 dB for both the arrays. Similarly, with

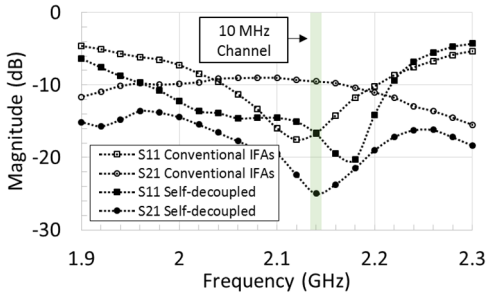

Fig. 14. Measured S-parameters of the self-decoupled antenna array and its IFA counterpart working at 2.14 GHz for MIMO OTA test.

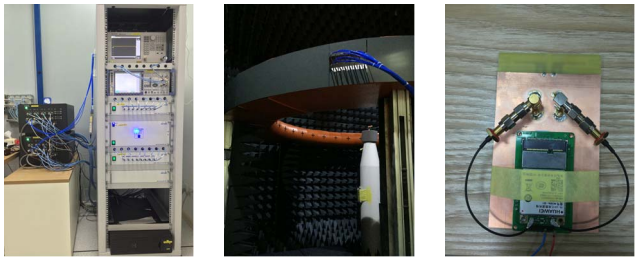

Fig. 15. MIMO OTA test facility. (a) Control equipment. (b) Multi-probe anechoic chamber. (c) MIMO LTE module integrated with an antenna array.

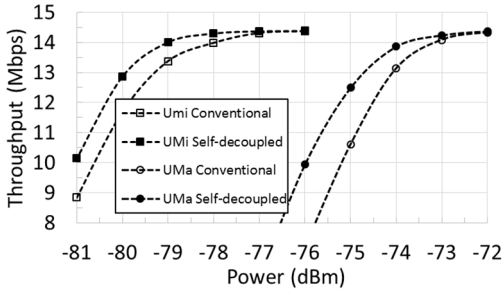

Fig. 16. Measured average throughputs versus power for the self-decoupled antenna array and its conventional IFAs counterpart with an MIMO module.

the first example, the measured total efficiency at 2.14 GHz is improved after using the proposed self-decoupled concept, with 73% for the self-decoupled antenna array and 65% for its conventional IFAs counterpart.

Each of these two antenna arrays is integrated with a commercially available two-port MIMO LTE module that supports 2.14 GHz (LTE band 1), individually, to constitute a complete communication device for the MIMO OTA test, as in a mobile phone. These two devices will be tested in a standard MIMO OTA test laboratory, which can provide controllable channel models, such as urban microcell (UMi) and urban macrocell (UMa) channel models. Fig. 15 shows the MIMO OTA test facility [20], [25].

In the MIMO OTA test, the duplex mode is the frequency division duplex (FDD) and the channel bandwidth is 10 MHz (2135–2145 MHz) with 16QAM modulation.

The average throughputs for the MIMO LTE module with the self-decoupled antenna array and the conventional IFAs counterpart under UMi and UMa channel models are compared in Fig. 16. Under the UMi channel, when the throughput drops to 13 Mbps (90% of the maximum value 14.386 Mbps), the required power for the MIMO module with the self-decoupled antenna array is about −79.9 dBm, while that with the conventional IFAs counterpart is about −79.3 dBm. The 0.6 dB reduction in the required power means that about 13% power saving can be achieved if the same data rate is retained. Similarly, about 0.7 dB (15%) power saving can be achieved under the UMa channel model.

IV. Conclusion

A new concept for enhancing the isolation of two antennas, namely, the self-decoupled antenna array, is proposed in this article. The working mechanism behind the new concept is revealed by a pertinent equivalent circuit model that incorporates the inductive and capacitive couplings. With the two opposite mutual couplings canceling out each other, the proposed antenna array can achieve inherently high isolation without introducing an extra decoupling structure between the antennas. It should be noted that the proposed self-decoupled antenna array occupies a slightly larger size compared with its traditional counterpart. But this issue can be overcome if a 3-D form realization for the additional branch is adopted. It could be a future work to study self-decoupled antennas in compact form. One possible direction is to use dielectric loading, and another is to cut slots on the antenna radiating arms to adjust the opposite couplings. A design guideline is drawn by parametric studies with EM simulations. The measured results show that two very closely placed antennas can achieve good return loss (better than 10 dB), high isolation (better than 20 dB), and low ECC (less than 0.07) across a wide frequency band (3.3–3.8 GHz). The data throughputs of an MIMO LTE module integrated with a pair of self-decoupled antennas and a pair of conventional IFAs are measured in the in-house MIMO OTA facility. The significant improvement on power saving for the same data throughput justifies the usefulness of the proposed self-decoupled antenna array for MIMO wireless terminals.

References

[1] M. A. Jensen and J. W. Wallace, "A review of antennas and propagation for MIMO wireless communications," *IEEE Trans. Antennas Propag.*, vol. 52, no. 11, pp. 2810–2824, Nov. 2004.

[2] X. Mei and K.-L. Wu, "How low does mutual coupling need to be for MIMO antennas," in *Proc. IEEE Int. Symp. Antennas Propag. USNC/URSI Nat. Radio Sci. Meeting*, Boston, MA, USA, Jul. 2018, pp. 1579–1580.

[3] H. Carrasco, H. D. Hristov, R. Feick, and D. Cofré, "Mutual coupling between planar inverted-F antennas," *Microw. Opt. Technol. Lett.*, vol. 42, no. 3, pp. 224–227, Jun. 2004.

[4] J. Holopainen, J.-M. Hannula, and V. Viikari, "A study of 5G antennas in a mobile terminal," in *Proc. 11th Eur. Conf. Antennas Propag. (EUCAP)*, Paris, France, Mar. 2017, pp. 3079–3081.

[5] F. Yang and Y. Rahmat-Samii, "Microstrip antennas integrated with electromagnetic band-gap (EBG) structures: A low mutual coupling design for array applications," *IEEE Trans. Antennas Propag.*, vol. 51, no. 10, pp. 2936–2946, Oct. 2003.

[6] C.-Y. Chiu, C.-H. Cheng, R. D. Murch, and C. R. Rowell, "Reduction of mutual coupling between closely-packed antenna elements," *IEEE Trans. Antennas Propag.*, vol. 55, no. 6, pp. 1732–1738, Jun. 2007.

[7] B. K. Lau and J. B. Andersen, "Simple and efficient decoupling of compact arrays with parasitic scatterers," *IEEE Trans. Antennas Propag.*, vol. 60, no. 2, pp. 464–472, Feb. 2012.

[8] L. Zhao and K.-L. Wu, "A decoupling technique for four-element symmetric arrays with reactively loaded dummy elements," *IEEE Trans. Antennas Propag.*, vol. 62, no. 8, pp. 4416–4421, Aug. 2014.

[9] H. Xu, H. Zhou, S. Gao, H. Wang, and Y. Cheng, "Multimode decoupling technique with independent tuning characteristic for mobile terminals," *IEEE Trans. Antennas Propag.*, vol. 65, no. 12, pp. 6739–6751, Dec. 2017.
[10] J. Andersen and H. Rasmussen, "Decoupling and descattering networks for antennas," *IEEE Trans. Antennas Propag.*, vol. 24, no. 6, pp. 841–846, Nov. 1976.
[11] J. Sui and K.-L. Wu, "A general T-Stub circuit for decoupling of two dual-band antennas," *IEEE Trans. Microw. Theory Techn.*, vol. 65, no. 6, pp. 2111–2121, Jun. 2017.
[12] A. Diallo, C. Luxey, P. Le Thuc, R. Staraj, and G. Kossiavas, "Study and reduction of the mutual coupling between two mobile phone PIFAs operating in the DCS1800 and UMTS bands," *IEEE Trans. Antennas Propag.*, vol. 54, no. 11, pp. 3063–3074, Nov. 2006.
[13] S.-W. Su, C.-T. Lee, and F.-S. Chang, "Printed MIMO-antenna system using neutralization-line technique for wireless USB-dongle applications," *IEEE Trans. Antennas Propag.*, vol. 60, no. 2, pp. 456–463, Feb. 2012.
[14] S.-C. Chen, Y.-S. Wang, and S.-J. Chung, "A decoupling technique for increasing the port isolation between two strongly coupled antennas," *IEEE Trans. Antennas Propag.*, vol. 56, no. 12, pp. 3650–3658, Dec. 2008.
[15] H. Meng and K.-L. Wu, "An LC decoupling network for two antennas working at low frequencies," *IEEE Trans. Microw. Theory Techn.*, vol. 65, no. 7, pp. 2321–2329, Jul. 2017.
[16] C. Volmer, J. Weber, R. Stephan, K. Blau, and M. A. Hein, "An eigenanalysis of compact antenna arrays and its application to port decoupling," *IEEE Trans. Antennas Propag.*, vol. 56, no. 2, pp. 360–370, Feb. 2008.
[17] L. Zhao, L. K. Yeung, and K.-L. Wu, "A coupled resonator decoupling network for two-element compact antenna arrays in mobile terminals," *IEEE Trans. Antennas Propag.*, vol. 62, no. 5, pp. 2767–2776, May 2014.
[18] K. Qian, L. Zhao, and K.-L. Wu, "An LTCC coupled resonator decoupling network for two antennas," *IEEE Trans. Microw. Theory Techn.*, vol. 63, no. 10, pp. 3199–3207, Oct. 2015.
[19] C.-D. Xue, X. Y. Zhang, Y. F. Cao, Z. Hou, and C. F. Ding, "MIMO antenna using hybrid electric and magnetic coupling for isolation enhancement," *IEEE Trans. Antennas Propag.*, vol. 65, no. 10, pp. 5162–5170, Oct. 2017.
[20] J. Sui and K.-L. Wu, "Self-curing decoupling technique for two Inverted-F antennas with capacitive loads," *IEEE Trans. Antennas Propag.*, vol. 66, no. 3, pp. 1093–1101, Mar. 2018.
[21] K.-L. Wong, C.-Y. Tsai, and J.-Y. Lu, "Two asymmetrically mirrored gap-coupled loop antennas as a compact building block for eight-antenna MIMO array in the future smartphone," *IEEE Trans. Antennas Propag.*, vol. 65, no. 4, pp. 1765–1778, Apr. 2017.
[22] A. Zhao and Z. Ren, "Multiple-input and multiple-output antenna system with self-isolated antenna element for fifth-generation mobile terminals," *Microw. Opt. Technol. Lett.*, vol. 61, no. 1, pp. 20–27, Nov. 2018.
[23] L. Sun, H. Feng, Y. Li, and Z. Zhang, "Compact 5G MIMO mobile phone antennas with tightly arranged orthogonal-mode pairs," *IEEE Trans. Antennas Propag.*, vol. 66, no. 11, pp. 6364–6369, Nov. 2018.
[24] R. G. Vaughan and J. B. Andersen, "Antenna diversity in mobile communications," *IEEE Trans. Veh. Technol.*, vol. VT-36, no. 4, pp. 147–172, Nov. 1987.
[25] Microwave Vision Group, Paris, France. *StarMIMO*. Accessed: Mar. 10, 2020. [Online]. Available: https://www.mvg-world.com/zh-hans/products?category=Antenna%20Measurement

Jiangwei Sui (Member, IEEE) received the B.S. degree in electronics engineering from the University of Science and Technology of China (USTC), Hefei, China, in 2014, and the Ph.D. degree from The Chinese University of Hong Kong, Hong Kong, in 2019.

He is currently with Vivo Communication Technology Company Ltd., Dongguan, China, as an Antenna Engineer. His current research interests include antenna theory, multi-input multi-output (MIMO) antennas, terminal antennas, and antenna array decoupling techniques for mobile communication systems.

Ke-Li Wu (Fellow, IEEE) received the B.S. and M.Eng. degrees from the Nanjing University of Science and Technology, Nanjing, China, in 1982 and 1985, respectively, and the Ph.D. degree from Laval University, Quebec, QC, Canada, in 1989.

From 1989 to 1993, he was a Research Engineer with McMaster University, Ontario, ON, Canada. He joined the Corporate Research and Development Division, COM DEV (now Honeywell Aerospace), Cambridge, ON, Canada, in 1993, where he was a Principal Member of Technical Staff. Since 1999, he has been with The Chinese University of Hong Kong, Hong Kong, where he is currently a Professor and the Director of the Radio frequency Radiation Research Laboratory. His current research interests include electromagnetic (EM)-based circuit domain modeling of high-speed interconnections, robot automatic tuning of microwave filters, decoupling techniques of multi-input multi-output (MIMO) antennas, and the Internet of Things technologies.

Dr. Wu is a member of the IEEE MTT-8 Subcommittee. He served as an Associate Editor for the IEEE TRANSACTIONS ON MTT from 2006 to 2009. He was a recipient of the 1998 COM DEV Achievement Award and the Asia–Pacific Microwave Conference Prize twice in 2008 and 2012, respectively.